

TOWARD RADIO DETECTION OF PEV NEUTRINOS ON THE CUBIC KILOMETER SCALE *

GEORGE M. FRICHTER

*Bartol Research Institute, University of Delaware
Newark, DE 19716, USA*

E-mail: frichter@lepton.bartol.udel.edu

JOHN P. RALSTON and DOUGLAS W. MCKAY

*Department of Physics and Astronomy, University of Kansas
Lawrence, KS 66045-2151, USA*

E-mail: ralston@kuphsx.phsx.ukans.edu

E-mail: mckay@kuphsx.phsx.ukans.edu

ABSTRACT

Interactions of ultrahigh energy neutrinos of cosmological origin in large volumes of radio-transparent South Polar ice can be detected via coherent Čerenkov emission from accompanying electromagnetic showers. A pilot experiment employing buried radio receivers has been successfully deployed at the South Pole and data are now being collected. The physics of coherent radio emission together with the properties of radio-pulse propagation in Antarctic ice clearly distinguishes the radio method from phototube detection. In the context of the proposed km³-scale neutrino telescope, these two detection modes provide *complementary* information on UHE neutrino interactions.

1. Introduction

The case has been made at this conference and elsewhere that the natural scale for ultra-high energy (UHE) neutrino astronomy is 1 km³ ^{1,2)}. Several groups are making significant progress toward the goal of “KM3” detection by employing smaller scale phototube arrays deep in lake or ocean water and Antarctic ice ²⁾. In the context of the overall KM3 effort, these efforts can be regarded as a proving grounds for detection strategies and associated technologies best suited to the task of “instrumenting a mountain”.

One promising detection strategy involves observing coherent radio Čerenkov emission ³⁾. The coherent effect is produced for frequencies up to the microwave region (few GHz) ⁴⁾ and results in a detection efficiency that scales with energy very differently compared with conventional phototube detection ^{5,6)}. Cold Antarctic ice is also remarkably transparent to electromagnetic (EM) radiation at frequencies below a few GHz, having attenuation lengths easily exceeding 1 kilometer ⁷⁾, whereas absorption at optical frequencies is about one order of magnitude less favorable. Scattering lengths for radio and optical frequencies also differ significantly, with virtually

*Conf. Proc. 7th International Symposium on Neutrino Telescopes, Feb. 27 - Mar. 1, 1996.

no volume scattering of long wavelength radiation expected. These factors lead one to consider seriously the potential complementarity of the two detection modes in the context of a KM3 detector located at the South Pole. In addition to the obvious advantage of independently observing events with detectors obeying different physics, unique kinematic information about simultaneously observed events is available which cannot be achieved by employing either detection mode separately.

As a step toward understanding the operation of radio detectors in the Antarctic, a pilot experiment has been deployed this season in two of the four AMANDA-B deep bore holes at the South Pole. In section 2, we discuss the elements of this deployment and describe its current status.

Section 3 is devoted to a discussion of the basic scaling relations for radio detection, and section 4 compares the overall efficiency of radio receivers and phototubes for detecting neutrino induced cascades. Important differences between the two methods and some new ideas for exploiting those differences in the context of a hybrid radio-phototube array are explored in section 5.

Much excitement in the field of UHE neutrino astronomy has been generated recently by the possibility that neutrinos from active galactic nuclei (AGN) may dominate the spectrum at energies above a few hundred TeV. Section 5 gives a detailed estimate for the neutrino event rate seen by a radio receiver buried deep in the Antarctic ice cap based on a theoretical model for the diffuse AGN flux.

2. RICE - A Pilot Radio Experiment[†]

Figure 1 indicates the main elements of the RICE 1995-96 deployment. The experiment consists of two deep radio receivers at depths of 250 meters and 150 meters, a surface mounted “trigger” receiver, a mobile transmitter, and finally a data acquisition system (DAQ) consisting of a 2 Giga-sample digital scope driven by a micro-computer. The receivers are connected to the DAQ by low loss coaxial transmission lines. Typical data samples collected on each channel are voltages sampled at 2 GHz over a 60 μ s time window, giving a very detailed record of received pulse shapes.

The radio receivers were designed with simplicity and survivability in mind. Each consists of a simple copper cylindrical dipole “tuned” such that the expected $\lambda/2$ resonance in ice (refractive index = 1.78) is about 130 MHz with a 3 dB bandwidth of 10 to 15 MHz. Each dipole is encased in a PVC/epoxy housing for good structural strength and low drag during deployment. Amplification of the signal to a level suitable for the trip up to the surface occurs by two low noise amplification stages (power gain: 36 dB each, 72 dB total) housed inside a steel pressure vessel. Power for each amplifier along with the amplified signal are carried on a single coax transmission line.

The mobile transmitter is capable of producing pulses with a center frequency of 120 MHz with a switchable bandwidth of 10 to 50 MHz. Given the limited bandwidth

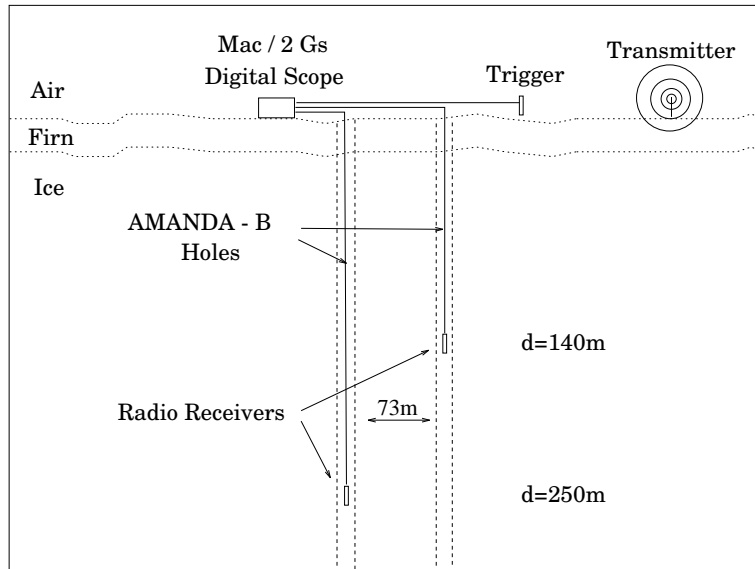


Fig. 1. 1995-96 RICE deployment: consists of three radio receivers (two deep, one on surface), one pulse transmitter (mobile), and a data acquisition system on the surface. Receivers are connected to the DAQ by low-loss transmission lines.

of the receivers, the shortest pulses will be useful for observing the “impulse response” of the receivers *in situ*. This is a key element in understanding the test results.

The scientific and technical goals of the current deployment can be summarized as follows.

- design and deploy radio receivers suited to the harsh Antarctic conditions - electronics must be water tight up to 1 km depth and able to survive overpressures which occur during refreeze, as well as temperatures in the -50° C range.
- observe coincident pulses on three data channels and characterize the response of the receivers using the transmitter.
- identify and characterize sources of ambient radio frequency noise in the south polar ice.

At the time of this conference, some two to three weeks after deployment of the two deep receivers, preliminary data have been collected and we can say that the first of these three goals has been achieved. The receivers have survived deployment and appear to be operating normally. At this very early stage, some key elements of the test remain to be deployed (the surface transmitter and the surface receiver), and we

eagerly await the results of the full test in the near future.

3. Basic Scaling Relations for Radio Detection

The efficiency for radio detection of neutrino induced EM cascades in ice scales very differently with energy compared to phototube detection. This fact can be understood by recalling the Frank-Tamm formula for Čerenkov power radiated per frequency per path length by a charge z , moving with speed $v = \beta c$, through a medium with refractive index n :

$$\frac{d^2W}{d\nu dl} = \left(\frac{4\pi^2\hbar}{c}\alpha_{\text{em}}\right)z^2\nu\left[1 - \frac{1}{\beta^2n^2}\right]. \quad (1)$$

We immediately see that the available signal power scales with frequency and the *square* of the charge involved. When considering the power radiated by all the charges in a large EM cascade, the high and low frequency limits display different behavior due to simple coherence effects. For wavelengths small compared with the spatial charge distribution, the phases of arriving Čerenkov wavelets from each particle are randomly distributed resulting in an incoherent sum of each contribution to the total observed power. In this case, the signal power scales with the total number of charged particles, which is given roughly by the shower energy E_s measured in GeV. At the opposite extreme, when wavelengths are large in comparison to the shower dimensions, wavelets arriving from charged particles are in phase, leaving a coherent sum of impulses from the showers' net charge. It is well known that EM showers in dense media develop a significant excess of negative charge mainly by Compton scattering of shower photons on atomic electrons (Bhabha scattering, Møller scattering, as well as e^+e^- annihilation also contribute to a lesser degree) ^{4,8)}. The detailed Monte Carlo simulation for EM cascades in ice developed by Zas, Halzen and Stanev (ZHS) ⁴⁾ reveals that the net charge developed by a large shower scales with energy like $z \sim .3E_s/\text{GeV}$. Equation (1) then says that the available signal power in the coherent regime is increasing as E_s^2 . Because of this difference in scaling behavior (E_s for photo-detection compared with E_s^2 for radio detection), at sufficiently large shower energies the power in the long-wavelength components of the Čerenkov signal will dominate.

At a distance R from the cascade the signal intensity varies with energy as E_s^2/R^2 due to spherical spreading. For a fixed detector threshold, we see that the maximum detection distance is proportional to the energy, $R_{\text{max}} \sim E_s$. The detection volume per detector then increases with the shower energy *cubed*, $V_{\text{det}} \sim E_s^3$. This is the naive expectation in the absence of signal absorption in the medium and geometric effects. Fortunately, absorption lengths for radio frequency pulses in ice at measured Antarctic temperatures are known to exceed 1 kilometer ⁷⁾, so that the basic E_s^3

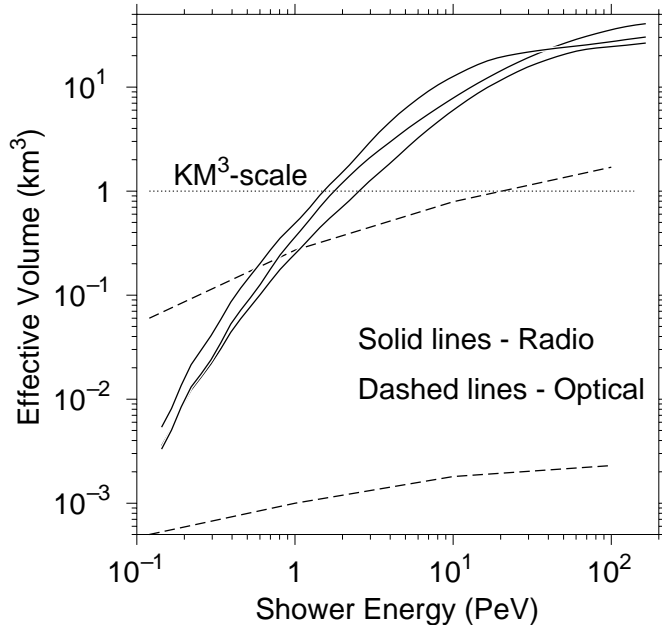


Fig. 2. Comparison of detection efficiencies of radio antennas versus phototubes. Optical estimates are from Ref. 6

scaling should hold up to volumes per radio receiver of order 1 km^3 .

4. Quantitative Efficiency Estimates

In a recent paper we performed detailed simulations based on a particular radio antenna and receiver which include all factors relevant to estimating detection efficiency and event rates (based on theoretical projections for diffuse neutrino fluxes)⁵. One important ingredient of those estimates is a parameterization of the signal spectrum (Fourier components of the time dependent electric field) given by the ZHS Monte Carlo⁴,

$$R|\vec{E}(\nu, R, \theta_c)| = \frac{0.55 \times 10^{-7}(\nu/\nu_o)}{1 + 0.4(\nu/\nu_o)^2} \frac{E_s}{1\text{TeV}} \exp\left[-\frac{1}{2}\left(\frac{\theta - \theta_c}{\theta_o} \frac{\nu}{\nu_o}\right)^2\right] \left(\frac{\text{V}}{\text{MHz}}\right), \quad (2)$$

where R is the distance between observer and cascade, $\nu_o = 500 \text{ MHz}$, $\theta_o \sim 2.4^\circ$, $\theta_c = 56^\circ$ is the Čerenkov angle in ice, and θ is the angle between the shower axis and

the observer. The target volume surveyed by a single radio receiver is an important measure of efficiency. By reciprocity, one can regard this also as the volume occupied by a detectable signal following a neutrino event. As the radio pulse propagates outward from the cascade site, it sweeps out a ‘fat’ conical volume, V_{signal} , set by the Čerenkov angle, the frequency-dependent angular half-width, $\Delta\theta = \theta_o\nu_o/\nu$, and the maximum range at which the pulse remains above threshold:

$$V_{\text{signal}} = \frac{4}{3}\pi R_{\text{max}}^3 \sin\theta_c \Delta\theta. \quad (3)$$

Choosing a typical frequency of 250 MHz gives a signal volume of 1 km³ when $R_{\text{max}} \sim 1.4$ km. The appropriate value for R_{max} depends on signal attenuation in the medium as well as the details of detector design.

Figure 2 compares effective detection volumes for a simple biconical antenna (‘tuned’ to 250 MHz) with a calculation of the same quantity for a 3 inch phototube ^{5,6}). The three solid curves show the radio efficiency for incident neutrino angles (with respect to vertical downward) of 120, 140 and 160 degrees (see figure 14 of reference ⁵). The lower and upper dashed curves are for photo-detection with and without ice bubbles ⁶). In the case of ice with bubbles, the radio and optical effective volumes are comparable near 100 TeV. A reasonably optimistic calculation of the case of ice with no bubbles shows comparable effective volumes near 800 TeV. In either event, radio becomes more efficient with increasing energy, exceeding either estimate of the phototube effective volume by at least a factor of 10 at 10 PeV.

5. Antennas and Phototubes: A Match Made In Heaven?

The roughly comparable volumes shown in Fig. 2 suggest that radio receivers and phototubes might be employed together as independent detection modes for a KM3 observatory, offering complementary information about neutrino events. At energies below 10-100 TeV, where phototube sensitivity dominates, the hybrid KM3 array would operate by observing mainly ν_μ induced muons passing through the arrayed volume. Above about 100 TeV the radio and optical modules will begin to survey increasingly large target masses surrounding the fiducial array volume (see Fig. 2) for neutrino induced cascades. Until now, the advantages of employing a hybrid radio-optical array have not been fully appreciated. In this section we hope to point out just a few of the interesting possibilities, focusing on electron neutrino events.

5.1. Background Rejection

One consequence of the poor radio efficiency for $E_s < 100$ TeV is that, compared with phototube detection, radio is relatively insensitive to unwanted backgrounds from local cosmic ray interactions (atmospheric neutrinos and muons) which have steeply falling spectra. In fact, our recent estimate indicates less than one back-

ground event per year from atmospheric neutrinos ⁵⁾. Radio-phototube coincidence introduces automatic energy discrimination that could be used to reject unwanted physics backgrounds.

5.2. Scattering, Event Geometry and Pulse Timing

The ability to “point” a neutrino telescope amounts to having reliable information on the geometry of observed events. This is clearly of fundamental importance to UHE neutrino astronomy. The ‘fat’ cone geometry described in section 4 together with pulse timing are key to obtaining good pointing accuracy from cascade observations. How this information is retained for radio versus optical frequency signals differs significantly due to the vast difference in the wavelengths involved (a factor of 10^6).

Having nicely macroscopic wavelengths (order meters), radio waves are expected to suffer no significant volume scattering as they propagate over kilometer distances. Macroscopic density variations should occur only in the uppermost 100 meters (firn layer) of ice, and will affect only a small fraction of potential event geometries. The net result is that radio pulses can retain good directional and timing information about the event even after propagating over large distances from interaction site to receiver.

In contrast, scattering opportunities for optical photons appear to be plentiful. Scattering in bubble-free ice at the South Pole is expected to be dominated by dust particles with a scattering length of about 20 meters (considerably less in dust bands) and a mean scattering angle of $\langle \cos(\theta) \rangle \sim 0.9$ ⁶⁾. The optical signal begins life with the sharp geometry of the original Čerenkov cone, but these photons then begin to diffuse, spreading out arrival times and eventually becoming isotropic on the KM3 scale. This clearly impacts pulse timing and geometry determination. However, the diffusing signal leads to improved detection thresholds because more phototubes per event will be ‘hit’ compared with a non-diffusing scenario.

The complementarity of combining optical and radio signals may lead to very interesting enhancements and deserves to be investigated in detail. For example, timing information supplied by the radio pulse may assist with photodetection, both by allowing thresholds to be adjusted advantageously and by knowing when to look in the photodetector output. It seems possible that distant events whose diffuse signal would be spread out too much in time for straight photodetection might be registered by using the extra information from the radio signal. More study of this, and attention to the substantial difference between electron and muon neutrino events is certainly needed.

An extremely interesting idea ⁹⁾ involves exploiting the different propagation speeds of radio and optical signals in ice. The refractive index for radio signals in ice is about 1.8 and about 1.3 for visible light. If there is no scattering (or if “leading” optical photons are detected ¹⁰⁾), then a signal 100 meters away from a co-located

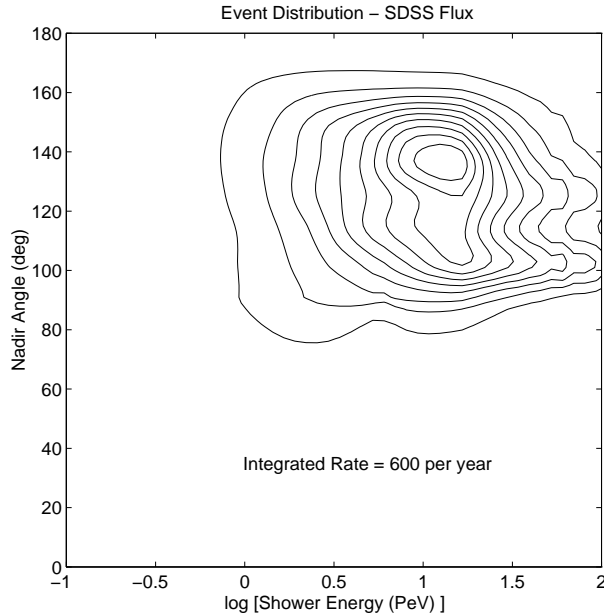


Fig. 3. The distribution of AGN neutrino events as detected by a single antenna located 500 meters below the ice surface using the SDSS flux prediction. We plot 10 equally spaced contours of the quantity $dN/d\cos\theta/d\log E$, with the ratio between the innermost and outermost contours equal to 10.

optical/radio detector arrives a “huge” 150 ns later in radio than in visible light. At 1 km event distance the timing difference becomes $1.5 \mu\text{s}$! If the timing resolution of the detectors is 10 ns, then the two arrival times determine the distance to the event vertex to within \pm ‘a few meters’. Evaluation of the usefulness of this phenomenon is, however, complicated by scattering and the resulting broadening of the optical component. We are investigating the use of these techniques not only to enhance detection, but also in conjunction with pulse height information to more accurately determine event energy ^{9,10}. The multiplicity of new “handles” from joining optical and radio detection is very exciting indeed.

6. Radio Event Rates - Diffuse AGN Prediction

Here we will briefly present some results for radio event rates based on models for the diffuse neutrino flux predicted for AGN; details can be found elsewhere ⁵. Figure (3) shows our result based on the model of Stecker *et al.* ¹² (SDSS) for a radio receiver buried 500 meters below the ice surface. The contours indicate constant event probabilities as a function of the shower energy (horizontal axis) and the incident angle for the incoming neutrino (vertical axis). Events are predicted to be clustered at energies between 1 and 50 PeV and angles between horizontal and about 60° above horizontal. Note that almost no neutrinos come from below the horizon due

to absorption in the Earth, except for a few events $< 20^\circ$ below the horizon at energies below 10 PeV. Although the angular distribution is skewed by the effects of absorption, the increased cross section at UHE yields an overall increase in total rate compared to earlier estimates ¹¹⁾. The total rate for the SDSS model is about 600 events per year per detector. An array of a few hundred radio detectors in a cubic kilometer volume would create a genuine radio neutrino telescope.

7. Summary

- A pilot experiment employing buried radio receivers in the Antarctic was successfully deployed at the South Pole this year.
- Differences between radio and phototube detection of UHE cascades result both from physics at the signal source and signal propagation in the medium. These differences present a unique opportunity to obtain *independent* information on event kinematics, improving the accuracy of geometry and energy estimation and extending the sensitivity of the KM3 observatories to higher energies.
- Diffuse neutrinos from AGN may produce large numbers of events in a radio array.

A unique opportunity exists for KM3 neutrino astronomy in the Antarctic. In polar ice we are indeed fortunate to have two complementary and comparably efficient detection modes available to observe neutrino induced cascades. The advantages of employing radio and phototube elements on the KM3-scale have only begun to be investigated. We believe that maximizing the ‘cost per unit science’ function will make a compelling case for hybrid radio-phototube arrays.

8. Acknowledgements

This work was supported in part under Department of Energy Grant Numbers DE-FGO2-85-ER 40214 and DE FG02 91 ER 40626.A007, and by the Kansas Institute for Theoretical and Computational Science.

† List of RICE Collaborators:

* Bartol Research Institute, Newark, DE 19716 USA

– George Frichter, Tim Miller, Lucio Piccirillo, David Seckel, Michele Limon

* University of Kansas, Lawrence, KS 66045-2151, USA

– Dave Besson, Alice Bean, Chris Allen, Sergei Kotov, Ilya Kravchenko, Suruj Seunarine

9. References

- 1) see F. Halzen these proceedings, also F. Halzen, in *Particle and Nuclear Astrophysics and Cosmology in the Next Millennium*, edited by E. W. Kolb and R. D. Peccei (World Scientific, Singapore, 1995).
- 2) T. Gaisser, F. Halzen and T. Stanev, Phys. Rep. **258**, 173 (1995).
- 3) M. Markov and I. Zheleznykh, Nucl. Instrum. Meth. Phys. Res. **A248**, 242 (1986); I. Zheleznykh, in *Proceedings of Neutrino '88*, Boston-Medford 1988, p. 528, edited by J. Schneps, T. Kafka and W. A. Mann (World Scientific 1989); I. Zheleznykh, in *Proceedings of the 21st International Cosmic Ray Conference*, Adelaide 1989, Vol. 6, p. 528-533.
- 4) E. Zas, F. Halzen and T. Stanev, Phys. Rev. **D 45**, 362 (1992).
- 5) G. M. Frichter, J. P. Ralston and D. W. McKay, Phys. Rev. **D 53**, 1684 (1996).
- 6) P. B. Price, to appear in *Astropart. Phys.* (1996).
- 7) V. V. Bogorodsky and V. P. Gavriilo, *Ice: Physical Properties*, Modern Methods of Glaciology (Leningrad, 1980); A. N. Salamantin *et al.*, in *Antarctic Committee Reports*, Vol. 24, 94 (Moscow, 1985).
- 8) H. R. Allan in *Progress in Elementary Particle and Cosmic Ray Physics*, edited by J. G. Wilson and S. A. Wouthuysen, North-Holland, Amsterdam (1971).
- 9) G. M. Frichter, in preparation.
- 10) P. C. Mock *et al.*, in *Proceedings of the XXIV International Cosmic Ray Conference*, Rome, Italy 1995, pp. 758.
- 11) G. M. Frichter, D. W. McKay and J. P. Ralston, Phys. Rev. Lett. **74**, 1508 (1995).
- 12) F. W. Stecker, C. Done, M. H. Salamon and P. Sommers, Phys. Rev. Lett. **66**, 2697; E (1992): *ibid* **69**, 2738.